Low-temperature behavior of two ternary lanthanide nickel carbides: Superconducting $LaNiC_2$ and magnetic $CeNiC_2$

V. K. Pecharsky and L. L. Miller
Ames Laboratory, Iowa State University, Ames, Iowa 50011-3020

K. A. Gschneidner, Jr.
Ames Laboratory and Department of Materials Science and Engineering, Iowa State University, Ames, Iowa 50011-3020

(Received 31 December 1997; revised manuscript received 17 March 1998)

A study of the magnetic properties and the heat capacity as functions of temperature and magnetic field of two ternary carbides $RNiC_2$, where $R=$La and Ce, confirms that $LaNiC_2$ becomes superconducting at $T_c=2.7$ K, and that $CeNiC_2$ orders antiferromagnetically below 18 K. $LaNiC_2$ is a conventional superconductor with a critical field of 900 Oe at $T=2$ K. $CeNiC_2$ obeys the Curie-Weiss law between 50 and 300 K showing the nearly full Ce^{3+} magnetic moment, $p_{\text{eff}}=2.47(1)\mu_B$, and has a negative paramagnetic Weiss temperature $\Theta_p=-18.3(8)$ K. A low net magnetic moment in the ordered state, which is far from saturation in a magnetic field of 5 T, is consistent with an antiferromagnetic ground state. Below 20 K $CeNiC_2$ shows multiple-step magnetic transitions at 18, 10, and 2.4 K. Both $LaNiC_2$ (in the normal state) and $CeNiC_2$ have the same electronic heat capacity, $\gamma=6.5(2)$ mJ/mol K^2, which is typical for many lanthanide-based intermetallic compounds. The Debye temperature of $LaNiC_2$ determined from the heat capacity in the normal state below 5.5 K is $\Theta_D=388(9)$ K. [S0163-1829(98)06425-X]

I. INTRODUCTION

The existence and the crystal structure of the ternary lanthanide-nickel carbides $RNiC_2$ were first reported for $R=$Y, La, Ce, and Pr by Bodak and Marusin.[1,2] Later, Semenenko *et al.*[3] and Jeitschko and Gerss[4] confirmed the earlier results and found that the $RNiC_2$ phases form with all other lanthanides except Pm and Eu. The compounds $RNiC_2$ ($R=$Y, La, Ce–Nd, Sm, Gd–Lu) crystallize in the orthorhombic $CeNiC_2$-type structure (space group $Amm2$), which is a derivative of the hexagonal AlB_2-type crystal structure.[1,4] Refinement of the occupancy of Ni and C sites for $R=$Dy revealed that the compound is essentially stoichiometric.[4]

Magnetic properties were studied for $R=$Y, Pr, Nd, and Gd–Tm,[5] where it was established that $YNiC_2$ has a low, temperature-independent susceptibility; $PrNiC_2$ and $HoNiC_2$ do not order down to 4.2 K; and the $RNiC_2$ phases ($R=$Nd, Gd, Tb, Dy, Er, and Tm) order antiferromagnetically at 7, 14, 25, 10, 8, and 8 K, respectively. There is no magnetic moment associated with Ni and, therefore, lanthanide atoms are the only magnetic species in $RNiC_2$ compounds. None of the alloys containing a magnetic rare-earth ion follows the Curie-Weiss law in the range 4.2–250 K, and a 2-T magnetic field was not strong enough to saturate the magnetization at 4.2 K thus yielding a saturation magnetization much lower than expected for R^{3+} ions.[5] These behaviors could be due to crystalline electric-field effects caused by the low symmetry of R-ion sites (mm).[5] The studies of the magnetic structure using low-temperature neutron powder diffraction for $R=$Pr, Nd, and Tb–Tm (Refs. 6–9) confirmed that (1) $PrNiC_2$ does not order magnetically down to 1.5 K, (2) if $HoNiC_2$ orders, it does so between 1.5 and 4.5 K, and (3) the other ternary carbides order antiferromagnetically below their respective Néel temperatures. These studies[6–9] also corroborate that in all cases, except $ErNiC_2$, the ordered magnetic moment is significantly smaller than that of the R^{3+} ion.

In this paper we present the results of magnetization and heat-capacity studies of the compounds $LaNiC_2$ and $CeNiC_2$. As we were completing our study, the superconductivity at $T_c=2.7$ K in $LaNiC_2$ (Ref. 10) and multiple-step magnetic ordering below $\sim$20 K in $CeNiC_2$ (Ref. 11) were reported.

II. EXPERIMENTAL PROCEDURES

The alloys with nominal composition, $LaNiC_2$ and $CeNiC_2$ (total weight $\sim$5 g), were prepared by arc melting the pure elements in an argon atmosphere near ambient pressure. The lanthanum [99.79 at. % (99.99 wt %) pure] and cerium [99.93 at. % (99.99 wt %) pure] used in this study were prepared by the Materials Preparation Center, Ames Laboratory. The major impurities (in at. %) in lanthanum were H (0.165 at. %), O (0.019 at. %), and N (0.013 at. %), and in cerium O (0.040 at. %), and C (0.015 at. %). Both nickel [99.4 at. % (99.94 wt %) pure] with the main impurities H (0.29 at. %), C (0.24 at. %), and O (0.01 at. %) and spectroscopically pure carbon (graphite) were purchased from commercial sources.

During arc melting the alloys were kept in a liquid state long enough for solid graphite to react with liquid metals. Next the alloys were remelted six more times with the button being turned over each time to ensure the sample's homogeneity. The total weight losses during arc melting were less than 0.5% and, therefore, the alloys' compositions were assumed to remain unchanged. Heat treatment was performed in helium-filled quartz tubes at 1000 °C for 7 days. The x-ray powder-diffraction measurements (Cu $K\alpha$ radiation, SCINTAG diffractometer) revealed that, within the accuracy of the method (typical second-phase detection limit of $\sim$5%),

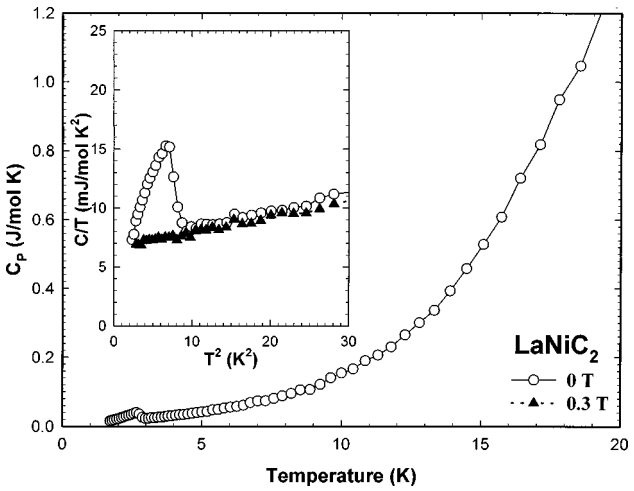

FIG. 1. The heat capacity of $LaNiC_2$ from 1.5 to 20 K in zero magnetic field. The inset shows C/T vs T^2 plots in zero magnetic field and in 0.3 T.

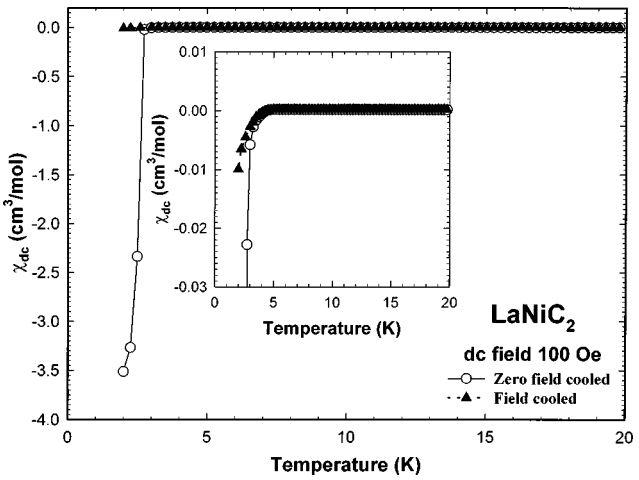

FIG. 2. The magnetic susceptibility of $LaNiC_2$ from 2 to 20 K measured in a weak magnetic field. The inset shows the magnetic susceptibility near the superconducting transition.

the heat-treated $LaNiC_2$ alloy contained only the orthorhombic $CeNiC_2$-type phase. A small amount of cerium dicarbide, CeC_2, was present in $CeNiC_2$ as the impurity phase (see Sec. III B and Fig. 5, below). The lattice parameters of $LaNiC_2$ and $CeNiC_2$ agree well with those reported earlier.[1–4]

The heat capacity from ~1.5 to 20 K in magnetic fields from 0 to 7.53 T and in zero magnetic field from ~1.5 to 60 K was measured using an adiabatic heat-pulse calorimeter described elsewhere.[12] The magnetic susceptibility was measured from 1.5 to 300 K in a 0.656-T field by using a Faraday microbalance.[13] The low-temperature, low-field dc magnetization was measured in a Quantum Design MPMS 5 dc magnetometer.

III. RESULTS AND DISCUSSION

A. Superconductivity of $LaNiC_2$

The heat capacity of $LaNiC_2$ in zero magnetic field from 1.5 to 20 K is shown in Fig. 1 with the C/T vs T^2 inset clarifying the low-temperature details. The sharp discontinuity between ~2.75 and 3 K is consistent with the transition to the superconducting state. The discontinuity in the heat capacity of $LaNiC_2$ in zero magnetic field, $\Delta C/\gamma T_c = 1.26$, indicates weak electron-electron coupling and confirms the bulk nature of superconductivity, although this quantity is slightly lower than the BCS theory prediction of ~1.43.[14]

The low-temperature (2–20 K), low-magnetic-field (100 Oe) magnetic susceptibility of $LaNiC_2$ is shown in Fig. 2. The strong diamagnetic signal below $T = 2.75$ K is temperature independent, and becomes weakly paramagnetic above ~4.5 K when the magnetic susceptibility was measured on warming (the sample was originally cooled to 2.0 K in a zero magnetic field), open symbols in Fig. 2. When the susceptibility was measured on warming after cooling the sample in a 100-Oe magnetic field, the diamagnetism is much weaker strongly suggesting magnetic-flux expulsion from the field-cooled sample. The behavior of the magnetic susceptibility (Fig. 2) is consistent with the zero-magnetic-field heat capacity (Fig. 1) indicating that a bulk superconducting transition occurs near $T_c = \sim 2.7$ K.

The effect of a magnetic field on the magnetization of $LaNiC_2$ at $T = 2$ K is shown in Fig. 3, which confirms the weak electron-electron coupling and indicates that the critical field at $T = 2$ K is near 0.09 T (900 Oe). Furthermore, the heat capacity measured in a 0.3-T magnetic field after the sample was cooled in zero field to ~1.5 K (inset of Fig. 1) shows that the critical field is below 0.3 T at $T = 1.5$ K (the lowest temperature in our experiment was 1.5 K). The fact that the 0.3-T magnetic field completely suppresses the superconducting transition permits one to obtain a reliable least-squares fit of the low-temperature heat capacity to determine the normal (nonsuperconducting) state electronic heat-capacity coefficient and the Debye temperature. As seen from the inset of Fig. 1, C/T behaves linearly as a function of T^2 from ~1.5 K ($T^2 = \sim 2.2$ K^2) to ~5.5 K ($T^2 = \sim 30$ K^2), and a linear least-squares fit yields the electronic heat-capacity coefficient $\gamma = 6.5(2)$ mJ/mol K^2, and the Debye temperature $\Theta_D = 388(9)$ K.

As mentioned above, the superconducting transition in $LaNiC_2$ at $T_c = 2.63$–2.86 K was reported recently by Lee

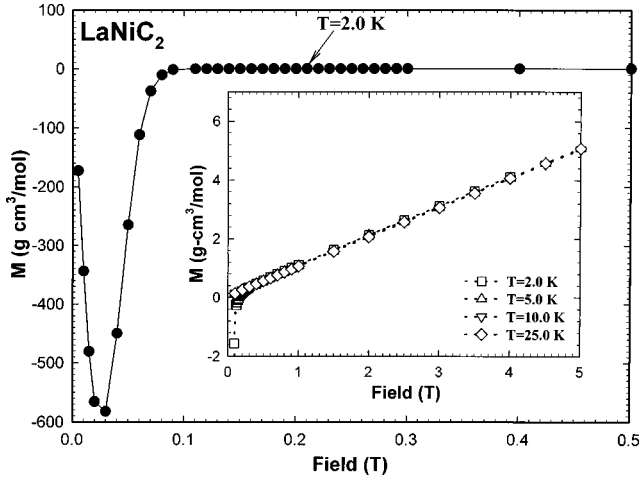

FIG. 3. The magnetization of $LaNiC_2$ at $T = 2.0$ K as a function of magnetic field in low fields (filled circles). The inset shows the magnetization as a function of magnetic field at $T = 2.0$, 5.0, 10.0, and 25.0 K in strong fields.

et al.[10] and our experimental results confirm this discovery. Our results, however, are different from those reported by Lee *et al.* with regard to the electronic heat-capacity coefficient (they gave 7.83 mJ/mol K^2) and the Debye temperature ($\Theta_D = 496$ K). This discrepancy is due to the fact that the least-squares fit was performed by Lee *et al.*[10] only using the heat-capacity values above the superconducting transition. This means that the extrapolation to $T^2 = 0$ is quite long (from $T^2 \cong 10\ K^2$) compared to our results (from $T^2 \cong 2.2\ K^2$) and this can lead to considerable inaccuracies. A close examination of the Fig. 1 inset shows that there is somewhat of an upward curvature for the heat-capacity results above $T^2 \cong 10\ K^2$ ($T \cong 3$ K). Fitting our heat-capacity data above $T^2 \cong 10\ K^2$ we obtain the values of $\gamma = 7.0(5)$ mJ/mol K^2 and $\Theta_D = 510(30)$ K, which are in much better agreement with the results of Lee *et al.*,[10] but still suffer from the long extrapolation (e.g., note the significantly increased uncertainties). Therefore, we deem that the electronic heat capacity of $\gamma = 6.5(2)$ mJ/mol K^2, and the Debye temperature of $\Theta_D = 388(9)$ K as being more accurate than the higher values reported by Lee *et al.*[10] for $LaNiC_2$.

The earlier work[10] concluded that $LaNiC_2$ is a nonconventional (i.e., non-BCS-type) low-temperature superconductor based on the nonexponential behavior of the electronic heat capacity C_{es} in the superconducting state. Our data show an exponential behavior of C_{es}, in agreement with the BCS theory[14] over the temperature range $1.52\ K \leqslant T \leqslant T_c$. The energy gap between the normal and the superconducting state, as determined from the intercept of the straight line, is $2\varepsilon_0/kT_c = 4.62$. However, our data do not extend far below T_c and, therefore, non-BCS behavior cannot be ruled out. It is also possible that the non-BCS behavior reported by Lee *et al.* is due to the errors in the Debye temperature, as noted above. Further experiments are necessary to determine whether $LaNiC_2$ is conventional or non-BCS, and whether it is a dirty type-I or a weak type-II superconductor.

B. Magnetism of $CeNiC_2$

As mentioned above, the x-ray powder diffraction revealed that the $CeNiC_2$ alloy used in our study contained a small amount of a second phase. This is apparent from the weak-diffraction peak near $2\Theta \cong 32.8°$ as marked by the arrow in Fig. 4. The position of this peak corresponds to the 110 reflection of the tetragonal CeC_2. It should be noted that this peak is the only one that is actually observed, although the 110 reflection is the second strongest peak in the CeC_2 x-ray-diffraction pattern (the strongest reflection, 011, should occur at ~26.8°, and is observed as a slight increase of the background; see Fig. 4). In general, it is impossible to identify the impurity phase from a single diffraction maximum. In this case, however, the magnetic ordering temperature of the impurity (see below) also corresponds to that of CeC_2. The reason for the presence of only one diffraction peak of the impurity phase is that there is a strong preferred orientation in the $CeNiC_2$ sample used in this powder-diffraction study. The texture axis of $CeNiC_2$ is the [100], and the texture parameter[15] is 0.17(1) (a value of 1.0 corresponds to the absence of preferred orientation). This indicates an almost sixfold increase in relative intensity of diffraction peaks that coincide with the texture axis. Assuming that the texture axis in the impurity phase is the [110], which is quite common for many tetragonal structures, the negligible intensity of the other strong reflections in CeC_2 (i.e., 011, 002, and 112) is expected. Because of all of the above, it is impossible to make an estimate of the amount of CeC_2 in the $CeNiC_2$ alloy from the x-ray powder-diffraction data. The magnetic entropy associated with the ordering of CeC_2 near 30 K (see below) is ~70 mJ/mol K. Compared with the theoretically available entropy for 1 mol of Ce^{3+} this yields to an estimated 0.5 mol % of CeC_2. The calculated concentration of the impurity is rather low; however, it further supports the suggestion that the CeC_2 phase is strongly textured, which permits its detection using x-ray powder diffraction.

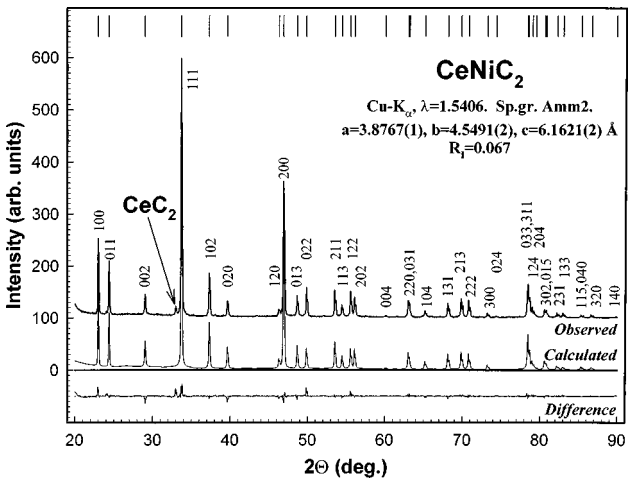

FIG. 4. Observed and calculated diffraction patterns of $CeNiC_2$ alloys together with the difference. Short vertical bars at the top of the figure indicate reflection positions. The arrow points to 110 reflection of the CeC_2 impurity.

The zero magnetic-field heat capacity from ~1.5 to 35 K of $CeNiC_2$ together with that of $LaNiC_2$, is shown in Fig. 5. It agrees well with that reported by Motoya *et al.*[11] The electronic heat-capacity coefficient and the Debye temperature cannot be determined by fitting the low-temperature heat capacity of $CeNiC_2$ in the usual way because the compound

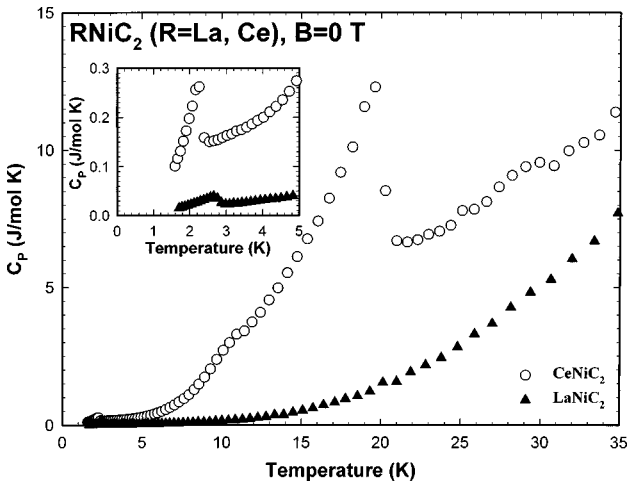

FIG. 5. The zero-magnetic-field heat capacity of $CeNiC_2$ and $LaNiC_2$ from ~1.5 to 35 K. The inset shows the details below 5 K.

orders magnetically at 2.4 K (see the inset of Fig. 5) and the magnetic contribution to the total heat capacity cannot be determined uniquely. However, one can estimate the electronic heat capacity of $CeNiC_2$ from the heat capacity of nonmagnetic $LaNiC_2$. Since the crystal structures of $CeNiC_2$ and $LaNiC_2$ are the same, and the atomic masses of Ce and La are close to one another, it is reasonable to assume that their respective Debye temperatures are quite close, i.e., $\Theta_D(LaNiC_2) \cong \Theta_D(CeNiC_2)$. Hence the difference in the heat capacity, if any, at a temperature above the magnetic phase transitions in $CeNiC_2$ (i.e., when the magnetic contribution to the total heat capacity becomes negligible) would be due to the difference in the electronic heat capacities of $CeNiC_2$ and $LaNiC_2$. Although not shown in Fig. 5, the heat capacities of both magnetic $CeNiC_2$ and nonmagnetic $LaNiC_2$ between 50 and 55 K become the same within the accuracy of experimental data, which indicates that the electronic heat-capacity coefficient of $CeNiC_2$ approaches that of $LaNiC_2$. The values of electronic heat capacity of both $CeNiC_2$ and $LaNiC_2$ [$\gamma = 6.5(2)$ mJ/mol K^2] are typical to those of common metallic materials. Thus the estimated value of the electronic heat capacity of $CeNiC_2$ (10 mJ/mol K) obtained by Motoya *et al.*[11] by fitting the lowest-temperature data (below $T = 2.2$ K) is in fair agreement with our results, but is less reliable because the magnetic contribution to the heat capacity was not taken into account.

The magnetic entropy of $CeNiC_2$, $S_{mag} = 8.34$ J/mol K, is $\sim 56\%$ of the theoretically expected value of $S_{mag} = R \ln(2J+1) = 14.9$ J/mol K, where R is the universal gas constant and J is the total angular momentum ($\frac{5}{2}$ for Ce^{3+}). This deficiency can be understood assuming that the magnetic order in $CeNiC_2$ is similar to that of the other members of the $RNiC_2$ series and that only 50% of Ce atoms order magnetically down to ~ 1.5 K. Lack of knowledge about crystalline electric field (CEF) levels in $CeNiC_2$, which may also contribute to the difference between theoretical and observed magnetic entropies, particularly when CEF levels are positioned far from the ordering temperature, prevents quantitative conclusions about the ordering in Ce sublattice.

The low-temperature details of the $CeNiC_2$ heat capacity are clarified in Fig. 6, where it is shown as C/T vs T plots in four different magnetic fields of 0, 2.46, 5.32, and 7.53 T. The lowest-temperature λ-type anomaly occurs at ~ 2 K in zero magnetic field and it is broadened and shifted to higher temperatures as the magnetic field increases, suggesting that the lowest-temperature magnetic phase is a ferromagnet or a ferrimagnet. The second (~ 10 K) heat-capacity anomaly is considerably broader (although it is heavily overlapped with next λ-type maximum) and remains practically unaffected by all magnetic fields. The strong λ-type heat-capacity maximum occurs at ~ 19 K and its position and height are also nearly magnetic field independent. This behavior of ~ 10 K and ~ 19 K heat-capacity anomalies is indicative of strongly coupled antiferromagnetic order in $CeNiC_2$ below ~ 19 K. These three heat-capacity anomalies agree well with the low-temperature magnetic susceptibility shown in Fig. 7. The highest temperature transition, which according to the magnetic susceptibility is antiferromagnetic and occurs at ~ 30 K (inset in Fig. 7), is practically invisible from the zero-magnetic-field heat-capacity data (Fig. 5) indicating that essentially no magnetic entropy is involved here. Recalling the presence of the impurity phase (see the beginning of this section), this leads to a conclusion that the upper temperature antiferromagnetic ordering occurs in the impurity phase rather than in the matrix. Earlier studies of magnetism in CeC_2 revealed that it orders antiferromagnetically at 30 K,[16,17] and therefore, strongly suggest that the impurity phase is CeC_2.

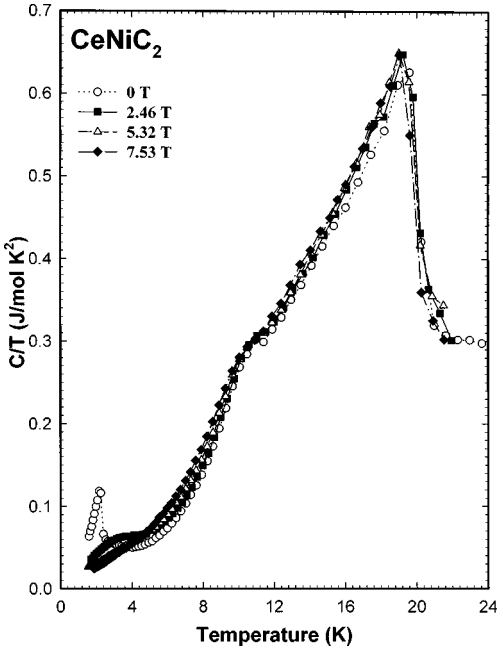

FIG. 6. Effect of the magnetic field on heat capacity of $CeNiC_2$ from ~ 1.5 to 20 K. The lines drawn through the data points are guides for the eye.

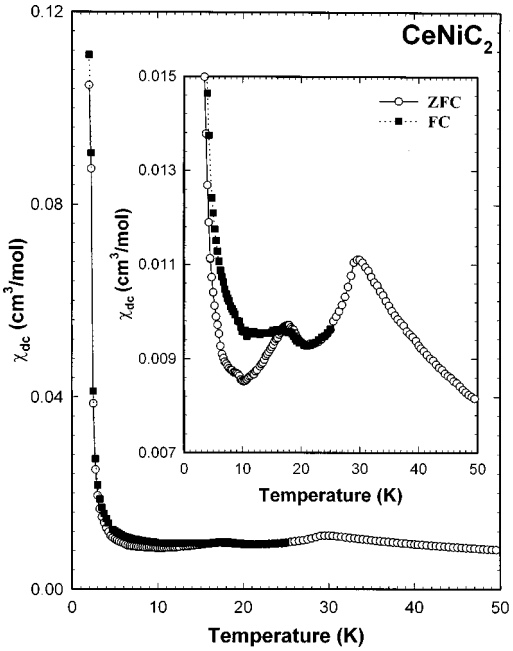

FIG. 7. Low-temperature magnetic susceptibility of $CeNiC_2$ measured in magnetic field of 0.01 T (100 Oe) on warming of the zero-magnetic-field-cooled sample (open circles) and on cooling in the same magnetic field (filled squares). The inset clarifies low-temperature details. Lines drawn through the data points are guides for the eye.

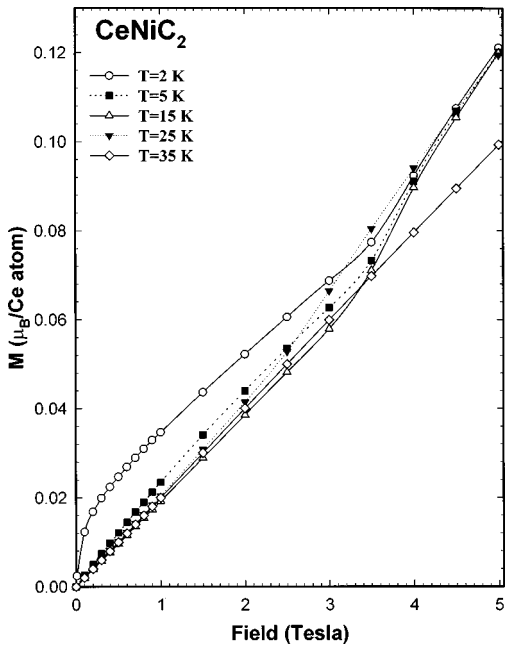

FIG. 8. Low-temperature magnetization of $CeNiC_2$ as a function of magnetic field at 2, 5, 15, 25, and 35 K.

The magnetic susceptibility of $CeNiC_2$ above ~ 50 K exhibits Curie-Weiss behavior. A linear least-squares fit yields an effective magnetic moment $p_{\mathrm{eff}}=2.47(1)\mu_B$, which is close to free-Ce^{3+}-ion value ($2.54\mu_B$), and a negative paramagnetic Curie temperature $\Theta_p=-18.3(8)$ K. The value of magnetic moment suggests that the Ce atoms are in their normal Ce^{3+} valence state, which agrees with smooth variation of the unit-cell volume in $R\mathrm{NiC}_2$ series.[3,4] This, combined with the weak Pauli paramagnetism of $LaNiC_2$ and the results of earlier studies of the magnetic properties of the other $R\mathrm{NiC}_2$ compounds,[5–9] confirms that Ni is nonmagnetic. The negative value of the paramagnetic Curie temperature is indicative of a negative exchange constant and antiferromagnetic ordering, at least in the high-temperature magnetic phase (also see below), and supports the conclusion made in the previous paragraph. The Curie-Weiss behavior and the presence of the full Ce^{3+} magnetic moment in the paramagnetic state of $CeNiC_2$ is in contrast to earlier reported almost temperature-independent susceptibility measured in a magnetic field of 0.01 T (100 Oe).[11]

The low-temperature magnetization behavior (Fig. 8) implies that the net magnetization in the ordered state of $CeNiC_2$ is extremely low. It is far from saturation and barely reaches 6% of that expected theoretically ($gJ=2.14\mu_B$ for Ce^{3+} ions) in a 5-T magnetic field. This is consistent with previously reported results for other members of $R\mathrm{NiC}_2$ series, where $R=$ Pr, Nd, Gd–Tm.[5–9] The magnetization behavior (Fig. 8) combined with the low-field susceptibility (Fig. 7) and heat-capacity (Figs. 5 and 6) data suggest that $CeNiC_2$ orders antiferromagnetically at 18 K. Simultaneously, the compound starts to exhibit a weak but obvious dependence of its magnetic susceptibility on the magnetic and thermal history of the sample below 18 K (Fig. 7). Typically, such behavior is indicative of spin-glass structures below their spin freezing temperature T_{sf} or of ferromagnets (ferrimagnets) below their Curie temperature T_C. It is doubtful that a spin-glass magnetic structure forms at 18 K since this is usually accompanied by a broad Schottky-type heat-capacity anomaly and not a sharp λ-type peak as in the case of $CeNiC_2$. Furthermore, there is no structural disorder of any kind in $CeNiC_2$, which is always present in known spin-glass systems. Hence, both magnetization and heat-capacity results indicate that the magnetic transition that occurs at 18 K most likely results in formation of antiferromagnetic structure that has a detectable ferromagnetic component causing the difference in the magnetic behavior of the zero-field-cooled and field-cooled samples.

The broader heat-capacity anomaly at 10 K corresponds to a small discontinuity in the magnetic susceptibility at 10 K, which is most pronounced in the zero-field-cooled sample measurement (Fig. 7, inset). Finally, a sharp upturn in the magnetic susceptibility, which begins near 3 K, corresponds to the lowest-temperature λ-type heat-capacity anomaly at 2.4 K. The field dependence of the magnetization at 2 K (Fig. 8) and heat capacity (Fig. 6) suggest that below 2.4 K the magnetic structure of $CeNiC_2$ has ferromagnetlike features, although some antiferromagnetic ordering may be present because of the extremely low net magnetization that is far from saturation in a field of 5 T. Magnetization data (Fig. 8) also show that between 2 and 25 K there is a magnetic-field-induced spin-flip transition that leads to the appearance of a ferromagneticlike behavior below 25 K when magnetic field exceeds 2.5–3.5 T. The critical field decreases from ~ 3.5 T at 2 K to ~ 3 T at 15 K, and to $\sim 2-2.5$ T at 25 K, and at all temperatures below ~ 25 K the magnetization becomes practically the same in fields higher than 4 T (Fig. 8).

The extremely low magnetization, and hence the very small changes in the net magnetization, accounts for the corresponding weak magnetic-field dependence of the heat capacity (Fig. 6). This is readily understood by recalling that the changes in magnetic entropy S_{mag} are related to the changes in magnetization as given by the Maxwell relation

$$(\partial S_{\mathrm{mag}}/\partial H)_T=(\partial M/\partial T)_H,$$

where H is the magnetic field strength, M is the magnetization, and T is the absolute temperature. Hence the effect of the magnetic field on the magnetic heat capacity C_{mag}, which is given as $C_{\mathrm{mag}}=T\partial S_{\mathrm{mag}}/\partial T$, is also small.

The total number and the temperatures of the observed magnetic-phase transitions in $CeNiC_2$ agree well with the results reported by Motoya *et al.*[11] Its magnetic structure was reported[11] to be most likely an incommensurate antiferromagnet between 10 and 18 K, which probably changes to commensurate antiferromagnet at ~ 10 K with quadrupling of the magnetic unit cell ($2a$, $2b$, c) compared to the crystallographic unit cell. Our results (three different ordering steps utilizing notably uneven amounts of magnetic entropy with the total being approximately equal to 50% of the theoretically available) support this conclusion. Assuming that the magnetic structure becomes incommensurate antiferromagnetic below ~ 18 K and that the modulation vector can easily change with temperature, this may account for multiple magnetic structures between 2.4 and 18 K and for different amounts of magnetic entropy associated with each of the three observed transitions.

IV. CONCLUSION

As a result of this study we confirm that the ternary carbide $LaNiC_2$ becomes superconducting at $T_c = 2.7$ K. Contrary to an earlier report of possible non-BCS superconductivity, it may be a conventional superconductor with a critical field of 900 Oe at $T = 2$ K.

The $CeNiC_2$ compound is characterized by a full Ce^{3+} magnetic moment in the paramagnetic region (from 50 to 300 K), but shows a low net magnetic moment in the ordered state that is far from saturation even in a magnetic field of 5 T and is consistent with an antiferromagnetic ground state. Below 20 K it shows multiple-step magnetic transitions at 18, 10, and 2.4 K. Most likely the magnetic structure of $CeNiC_2$ is an incommensurate antiferromagnetic below 18 K and the change in temperature leads to a change in the modulation vector or to a transition to a commensurate antiferromagnetic structure. Below 18 K there is an apparent hysteresis of the magnetic susceptibility, which is indicative of a weak ferromagnetic component in the antiferromagnetic structure of $CeNiC_2$. Both $LaNiC_2$ (in the nonsuperconducting state) and $CeNiC_2$ have the same electronic heat capacity, $\gamma = 6.5(2)$ mJ/mol K^2. The Debye temperature $\Theta_D = 388(9)$ K is quite high and it is probably associated with the presence of strongly covalently bonded C_2 pairs in the crystal structure.[1,4]

ACKNOWLEDGMENTS

The Ames Laboratory is operated by the U.S. Department of Energy by Iowa State University under Contract No. W-7405-ENG-82. This work was supported by the Office of Basic Energy Sciences, Materials Sciences Division. The authors also wish to thank Professor John Clem, Ames Laboratory and Department of Physics and Astronomy, Iowa State University for his comments.

[1] O. I. Bodak and E. P. Marusin, Dopov. Akad. Nauk. Ukr. RSR, Ser. A: Fiz.-Mat. Tekh. Nauki **1979**, 1048.

[2] O. I. Bodak and E. P. Marusin, in *Phase Diagrams of Refractory Systems*, edited by V. N. Eremenko (Institute of Problems in Materials Sciences, Metallurgiya, Kiev, 1980), p. 176 (in Russian).

[3] K. N. Semenenko, A. A. Putyatin, I. V. Nikol'skaya, and V. V. Burnasheva, Russ. J. Inorg. Chem. **28**, 943 (1983).

[4] W. Jeitschko and M. H. Gerss, J. Less-Common Met. **116**, 147 (1986).

[5] P. Kotsanidis, J. K. Jakinthos, and E. Gamari-Seale, J. Less-Common Met. **152**, 287 (1989).

[6] W. Shäfer, G. Will, J. K. Jakinthos, and P. Kotsanidis, J. Alloys Compd. **180**, 251 (1992).

[7] J. K. Jakinthos, P. Kotsanidis, W. Shäfer, and G. Will, J. Magn. Magn. Mater. **89**, 299 (1990).

[8] J. K. Jakinthos, P. Kotsanidis, W. Shäfer, and G. Will, J. Magn. Magn. Mater. **81**, 163 (1989).

[9] J. K. Jakinthos, P. Kotsanidis, W. Shäfer, and G. Will, J. Magn. Magn. Mater. **102**, 71 (1991).

[10] W. H. Lee, H. K. Zeng, Y. D. Yao, and Y. Y. Chen, Physica C **266**, 138 (1996).

[11] K. Motoya, K. Nakaguchi, N. Kayama, K. Inari, J. Akimitsu, K. Izawa, and T. Fujita, J. Phys. Soc. Jpn. **66**, 1124 (1997).

[12] K. Ikeda, K. A. Gschneidner, Jr., B. J. Beaudry, and U. Atzmony, Phys. Rev. B. **25**, 4604 (1982).

[13] R. J. Stierman, K. A. Gschneidner, Jr., T.-W. E. Tsang, F. A. Schmidt, P. Klavins, R. N. Shelton, J. Queen, and P. Legvold, J. Magn. Magn. Mater. **36**, 249 (1983).

[14] J. Bardeen, L. N. Cooper, and J. R. Schrifer, Phys. Rev. **106**, 162 (1957); **108**, 1175 (1957).

[15] V. K. Pecharsky, L. G. Akslerud, and P. Yu. Zavalij, Kristallografiya **32**, 343 (1987) [Sov. Phys. Crystallogr. **32**, 514 (1987)].

[16] T. Sakai, G. Adachi, and J. Shiokawa, J. Appl. Phys. **50**, 3592 (1979).

[17] T. Sakai, G. Adachi, and J. Shiokawa, Mater. Res. Bull. **15**, 1001 (1980).